Laser and Particle Beams (2009), *27*, 471–474. Printed in the USA.

doi:10.1017/S026303460999019X

Generation of strong magnetic fields from laser interaction with two-layer targets

S.Z. WU,[1] C.T. ZHOU,[2,3] X.T. HE,[2,3] AND S.-P. ZHU[2]

[1]Graduate School of the Chinese Academy of Engineering Physics, Beijing, People's Republic of China
[2]Institute of Applied Physics and Computational Mathematics, Beijing, People's Republic of China
[3]Center for Applied Physics and Technology, Peking University, Beijing, People's Republic of China

(RECEIVED 30 March 2009; ACCEPTED 10 May 2009)

Abstract

A two-layer target irradiated by an intense laser to generate strong interface magnetic field is proposed. The mechanism is analyzed through a simply physical model and investigated by two-dimensional particle-in-cell simulation. The effect of laser intensity on the resulting magnetic field strength is also studied. It is found that the magnetic field can reach up to several ten megagauss for laser intensity at 10^{19} Wcm^{-2}.

Keywords: Electron beams; Intense laser-plasma interaction; PIC simulation; Strong magnetic field

1. INTRODUCTION

The self-generated magnetic field (Stamper *et al.*, 1971; Sudan, 1993; Tatarakis *et al.*, 2002; Wu *et al.*, 2009; Zhou & He, 2008*a*, 2008*b*) during laser-plasma interaction has been widely investigated theoretically and experimentally over the past decades, because of many potential applications (Ghoranneviss *et al.*, 2008; Hora *et al.*, 1984, 2002, 2008*b*; Hora & Hoffmann, 2008*a*; Tan & Min, 1985; Zhou & He, 2007*a*, 2007*b*, 2007*c*), such as in fusion science, beam collimation, and electron acceleration, etc. When ultra-intense ($>10^{18}$ Wcm^{-2} μm^{-2}) lasers interact with overdense or solid targets, relativistic electrons are generated at the relativistic critical density. These fast electron currents will penetrate into the target and become a source of strong magnetic field, which can be up to 100 megagauss (MG) for laser intensities of 10^{20} Wcm^{-2}.

Recently, there have been works on the generation and application of strong interface magnetic fields. With specially designed target structures, both hybrid-Vlasov-Fokker-Planck (HVFP) (Robinson *et al.*, 2007) and hybrid-fluid-particle-in-cell (HFPIC) (Zhou *et al.*, 2008*a*, 2008*b*) simulations show that strong interface magnetic fields are generated because of the gradients in the resistivity and density at the material interface. However, in realistic experiments and applications, the fast electrons are generated during the laser-plasma interaction (LPI). The earlier HVFP or HFPIC simulations cannot consider this process directly. Instead, in these simulations, the electron beams are injected and are assumed to satisfy certain scaling law (Wilks *et al.*, 1992). By making use of the explicit two-dimensional particle-in-cell (PIC) simulation and including the LPI directly, here we investigate the generation of strong interface magnetic fields in a two-layer target irradiated by ultra-intense lasers. The effect of the laser intensity on the field strength is also studied. It is found that the interface magnetic field can reach up to tens MG for laser intensity at 10^{19} Wcm^{-2}, and even hundreds of MG for 10^{20} Wcm^{-2}.

2. PHYSICAL MODEL

The self-generated magnetic field from the intense laser-produced fast electron flux is given by (Bell *et al.*, 1998): $\partial \mathbf{B}/\partial t = \eta \nabla \times \mathbf{j}_f + \nabla \eta \times \mathbf{j}_f$, where $\mathbf{j}_f$ is the fast electron current density, and η is the space-dependent resistivity. Since the standard explicit PIC simulation cannot include the effect of resistivity, the magnetic field is due to the density gradient alone.

We now consider the target shown in Figure 1. It consists of two plasma layers of different densities (layers 1 and 2 with densities n_1 and n_2, respectively). For laser-driven electron beam with currents larger than the Alfvén limit, a return current $\mathbf{j}_r$ moving in the opposite direction will be induced to establish charge and current equilibrium. The local net current density is thus $\mathbf{j}_{\text{net}} \equiv \mathbf{j}_r + \mathbf{j}_f \sim \mu_0^{-1} \nabla \times \mathbf{B}$,

Address correspondence and reprint requests to: C.T. Zhou, Institute of Applied Physics and Computational Mathematics, P. O. Box 8009, Beijing 100088, People's Republic of China. E-mail: zcangtao@iapcm.ac.cn

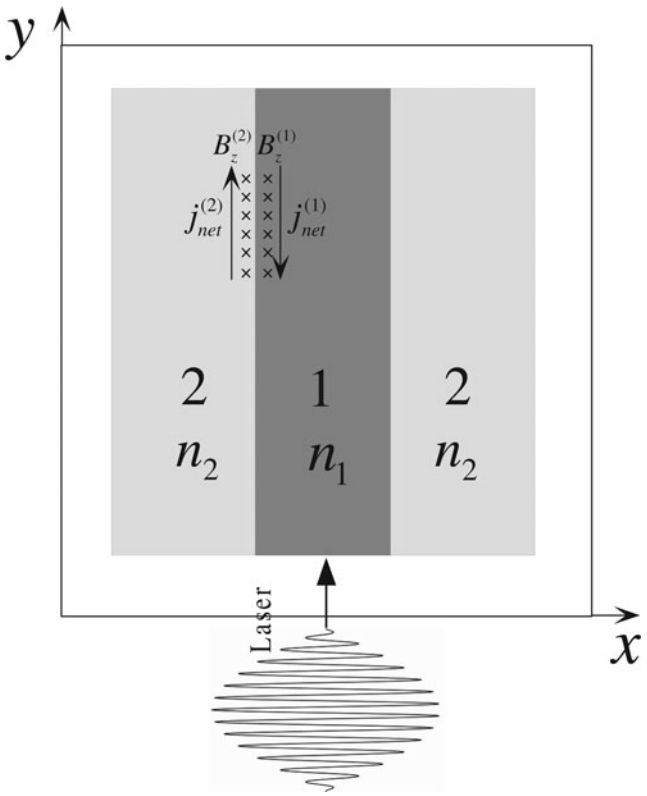

Fig. 1. A laser pulse incident on a two-layer target (layers 1 and 2 with plasma densities n_1 and n_2, respectively), and the self-generated interface magnetic field.

corresponding to $\mathbf{I}_A \approx 17.1\ \beta\gamma$kA (Batani *et al.*, 2002) in a width on the order of 0.1 μm.

The net currents on the two sides of the interface are different due to the density difference, but as a whole, there is a current balance: $j_{\text{net}}^{(1)} \sim -j_{\text{net}}^{(2)}$ (see Fig. 1). Therefore, a magnetic field $B_z = B_z^{(1)} + B_z^{(2)}$ will be generated near the interface according to Ampere's Law. We can write

$$B_z \sim \mu_0 j_{\text{net}}^{(1)} L_1 + \mu_0 j_{\text{net}}^{(2)} L_2, \tag{1}$$

where L_i ($i = 1, 2$) is the transverse width of the current. The fast electron current j_f can be estimated from the scaling law (Wilks *et al.*, 1992):

$$j_f = \frac{\eta_a I_{L,18}}{0.511\left(\sqrt{1 + I_{L,18}\lambda_0^2/1.38} - 1\right)}, \tag{2}$$

where $I_{L,18}$, λ_0, j_f represent the laser intensity, wavelength, and current density, in units of 10^{18} Wcm^{-2}, μm, and 10^{12} Acm^{-2}, respectively, and η_a is the laser absorption rate. For a typical intensity of $I_L = 10^{19}$ Wcm^{-2} and 30% absorption rate, the magnetic field strength can reach more than 30 MG according to Eqs. (1) and (2). It is also expected that the field strength will increase with increasing incident laser intensity.

3. SIMULATION RESULTS

Since we are mainly interested in the generation of the interface magnetic field by the density effect, the standard two-dimensional PIC technique is sufficient (Birdsall & Langdon, 1985). Our target configuration is shown in Figure 1. The two-dimensional (x, y) simulation box is 20 μm × 20 μm. The mesh resolution is 1200 × 1200 cells with 50 electrons and 50 ions in each cell. The initial temperature of the plasma electrons and ions is 1 keV. As shown in Figure 1, there are vacuum regions on the four sides of the target, 1 μm in the left and the right sides of the plasma (in the x direction), 2 μm in the front, and 1 μm behind the target (in the y direction). The periodic boundary condition is used in the x direction and the outgoing boundary condition in the y direction. The width of the inner layer (layer 1) is 4 μm in the x direction. The laser is incident from the bottom along the y direction with a rise time of about 4 fs, after which it remains at the constant peak intensity. The laser transverse profile (along the x direction) is super-gaussian with a 2.4 μm spot size. The laser wavelength is chosen to be $\lambda = 1.05$ μm.

We now consider two cases. The peak intensity of the incident laser is $I_L = 10^{19}$ Wcm^{-2} in case I, and 6×10^{19} Wcm^{-2} in case II. The target density profiles for the two cases are the same: $n_1 = 20n_c$, $n_2 = 50n_c$, where n_c is the critical density.

Figures 2a and 2c show the net current density and the corresponding magnetic field at $t = 160$ fs for case I. It is clearly seen that the net currents on the two sides of the interface have opposite signs, and the values are up to the order of 10^{12} Acm^{-2}. Such strong opposite currents generate a strong magnetic field along the interface (see Fig. 2c). In case I, the interface magnetic field can be more than 30 MG. The similar net currents and interface magnetic fields also appear in case II, as shown in Figures 2b and 2d. It is noted that the values for the current and magnetic field in case II are much larger than that in case I, as shown in Figure 2. According to Eqs. (1) and (2), higher laser intensity will generate higher current, and thus higher magnetic field.

In order to show the effect of laser intensity on the interface magnetic generation more quantitatively, several other cases have also been considered: 2×10^{19} Wcm^{-2}, 4×10^{19} Wcm^{-2}, 8×10^{19} Wcm^{-2}, and 10^{20} Wcm^{-2}. The other simulation parameters are identical to these in cases I and II. The strength of the resulting magnetic fields as a function of the incident laser intensity is shown in Figure 3. The line with the error bars is from the simulation, confirming that the field strength increases with the laser intensity. The analytical estimate based on Eqs. (1) and (2) is given in Figure 3 by the line with triangles. The good agreement demonstrates that the simple physical model is useful for estimating the interface magnetic field strength.

4. SUMMARY

To summarize, we have proposed a two-layer target for generating strong interface magnetic fields. The scheme is

https://doi.org/10.1017/S026303460999019X Published online by Cambridge University Press

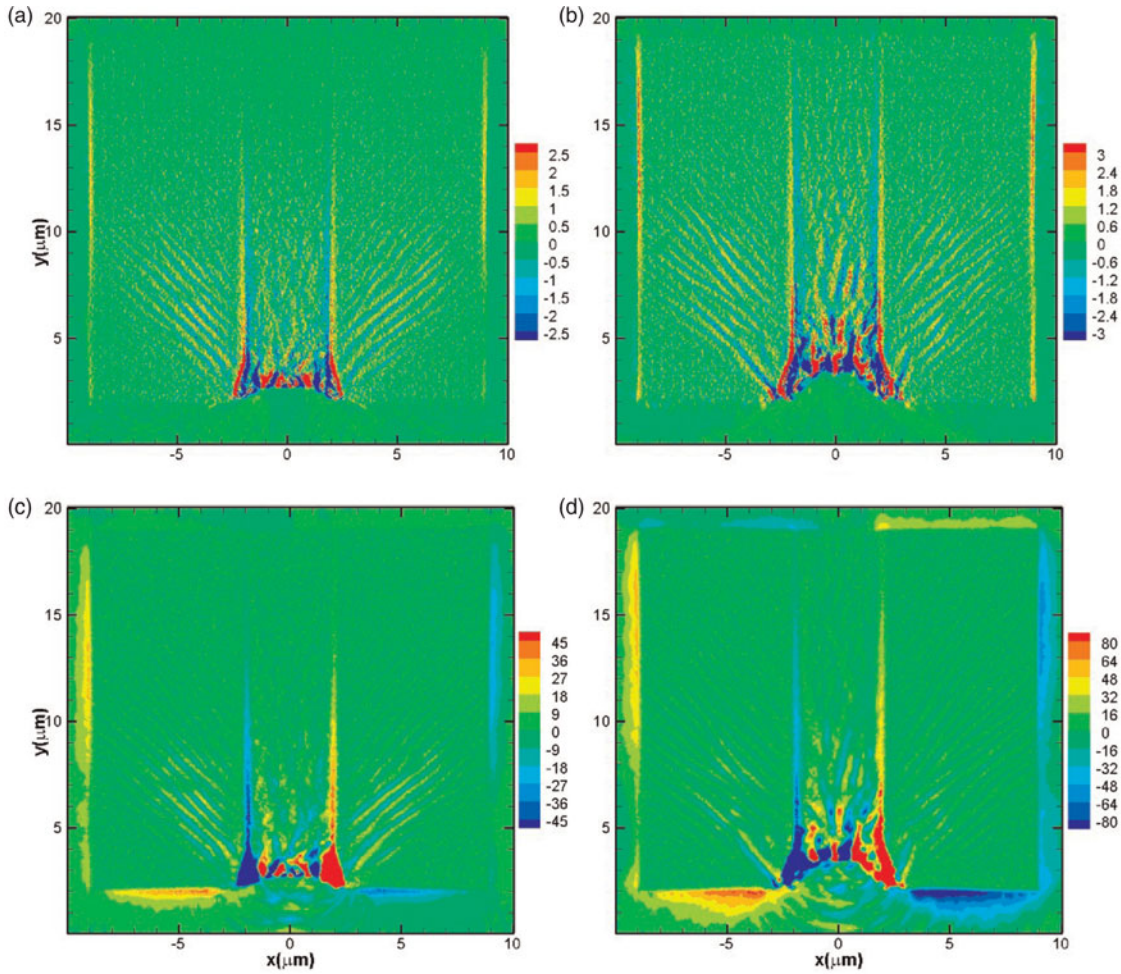

Fig. 2. (Color online) The net current density in the y direction j_{net} (in 10^{12} Acm^{-2}) at 160 fs: (**a**) for case I and (**b**) case II. The corresponding magnetic fields B_z (in MG): (**c**) case I and (**d**) case II.

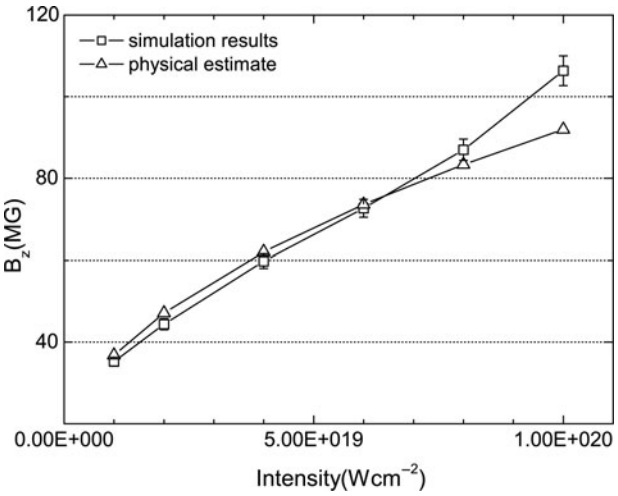

Fig. 3. The interface magnetic field B_z (in MG) against the incident laser intensity: simulation results (squares with the error bars) and physical estimate from Eqs. (1) and (2) (the line with triangles).

analyzed with a simple analytical model and the process is investigated using two-dimensional PIC simulation. It is found that the interface field can reach several tens MG at laser intensities of 10^{19} Wcm^{-2}. Furthermore, we have also studied the effect of laser intensity on the magnetic field strength. Our simulation results agree very well with that from the analytical model. Thus, the proposed scheme as well as the physical model should be useful in the applications such as in fast electron collimation and high energy density physics, where strong magnetic fields are required.

ACKNOWLEDGMENTS

Wu would like to thank Z.J. Liu for his helpful discussions on PIC simulation. This work is supported by the National Natural Science Foundation of China Grant Nos. 10835003 and 10575013 and the National High-Tech ICF Committee and partially by the National Basic Research Program of China (973)(2007CB815101).

https://doi.org/10.1017/S026303460999019X Published online by Cambridge University Press

REFERENCES

Batani, D. (2002). Transport in dense matter of relativistic electrons produced in ultra-high-intensity laser interactions. *Laser Part. Beams* **20**, 321–336.

Bell, A.R., Davies, J.R. & Guérin, S.M. (1998). Magnetic field in short-pulse high-intensity laser-solid experiments. *Phys. Rev. E* **58**, 2471–2473.

Birdsall, C.K. & Langdon, A.B. (1985). *Plasma Physics via Computer Simulation*. New York: McGraw-Hill Inc.

Ghoranneviss, M., Malekynia, B., Hora, H., Miley, G.H. & He, X.T. (2008). Inhibition factor reduces fast ignition threshold of laser fusion using nonlinear force driven block ignition. *Laser Part. Beams* **26**, 105–111.

Hora, H., Lalousis, P. & Eliezer, S. (1984). Analysis of the inverted double-layers produced by nonlinear forces in laser-produced plasmas. *Phys. Rev. Lett*. **53**, 1650–1652.

Hora, H., Hoelss, M., Scheid, W., Wang, J.X., HO, Y.K., Osman, F. & Castillo, R. (2000). Principle of high accuracy of the nonlinear theory for electron acceleration in vacuum by lasers at relativistic intensities. *Laser Part. Beams* **18**, 135–144.

Hora, H. & Hoffmann, D.H.H. (2008*a*). Using petawatt laser pulses of picosecond duration for detailed diagnostics of creation and decay processes of B-mesons in the LHC. *Laser Part. Beams* **26**, 503–505.

Hora, H., Malekynia, B., Ghoranneviss, M., Miley, G.H. & He, X.T. (2008*b*). Twenty times lower ignition threshold for laser driven fusion using collective effects and the inhibition factor. *Appl. Phys. Lett*. **93**, 0111011-3.

Robinson, A.P.L. & Sherlock, M. (2007). Magnetic collimation of fast electrons produced by ultraintense laser irradiation by structuring the target composition. *Phys. Plasams* **14**, 083105.

Stamper, J.A., Papadopoulos, K., Sudan, R.N., Dean, S.O., McLean, E.A. & Dawson, J.M. (1971). Electron acceleration by high current-density relativistic electron bunch in plasmas. *Laser Part. Beams* **26**, 1012–1015.

Sudan, R. (1993). Mechanism for the generation of 109 G magnetic fields in the interaction of ultraintense short laser pulse with an overdense plasma target. *Phys. Rev. Lett*. **70**, 3075–3078.

Tan, W. & Min, G. (1985). Thermal flux limitation and thermal conduction inhibition in laser plasmas. *Laser Part. Beams* **3**, 243–250.

Tatarakis, M., Watts, I., Beg, F.N., Dangor, A.E., Krushelnick, K., Wagner, U., Norreys, P.A. & Clark, E.L. (2002). Measurements of ultrastrong magnetic fields during relativistic laserïplasma interactions. *Phys. Plasmas* **9**, 2244.

Wilks, S.C., Kruer, W.L., Tabak, M. & Langdon, A.B. (1992). Absorption of ultra-intense laser pulses, *Phys. Rev. Lett*. **69**, 1383–1386.

Wu, S.Z., Liu, Z.J., Zhou, C.T. & Zhu, S.P. (2009). Density effects on collimation of energetic electron beams driven by two intense laser pulses. *Phys. Plasmas* **16**, 043106.

Yu, M.Y. & Luo, H.Q. (2008). A note on the multispecies model for identical particles. *Phys. Plasmas* **15**, 024504.

Zhou, C.T. & He, X.T. (2007*a*). Influence of a large oblique incident angle on energetic protons accelerated from solid-density plasmas by ultraintense laser pulses. *Appl. Phys. Lett.* **90**, 031503.

Zhou, C.T., Yu, M.Y. & He, X.T. (2007*b*). Electron acceleration by high current-density relativistic electron bunch in plasmas. *Laser Part. Beams* **25**, 313–319.

Zhou, C.T. & He, X.T. (2007*c*). Intense laser-driven energetic proton beams from solid density targets. *Opt. Lett.* **32** 2444–2446.

Zhou, C.T. & He, X.T. (2008*a*). Intense-laser generated relativistic electron transport in coaxial two-layer targets., *Appl. Phys. Lett.* **92**, 0715021-3.

Zhou, C.T. & He, X.T. (2008*b*). Laser-produced energetic electron transport in overdense plasmas by wire guiding. *Appl. Phys. Lett.* **92**, 1515021-3.

https://doi.org/10.1017/S026303460999019X Published online by Cambridge University Press